



# Application of honey-bee mating optimization on state estimation of a power distribution system including distributed generators

Taher NIKNAM

(Electronic and Electrical Department, Shiraz University of Technology, Shiraz, Iran)

E-mail: nikanam@sutech.ac.ir; taher\_nik@yahoo.com

Received Jan. 17, 2008; revision accepted Mar. 24, 2008; CrossCheck deposited Oct. 27, 2008

**Abstract:** We present a new approach based on honey-bee mating optimization to estimate the state variables in distribution networks including distributed generators. The proposed method considers practical models of electrical equipments such as static var compensators, voltage regulators, and under-load tap changer transformers, which have usually nonlinear and discrete characteristics. The feasibility of the proposed approach is demonstrated by comparison with the methods based on neural networks, ant colony optimization, and genetic algorithms for two test systems, a network with 34-bus radial test feeders and a realistic 80-bus 20 kV network.

**Key words:** Distributed generators (DGs), State estimation, Honey-bee mating optimization (HBMO)

**doi:**10.1631/jzus.A0820047

**Document code:** A

**CLC number:** TM921

## INTRODUCTION

Online monitoring plays a key role in improving the efficiency and reliability of a power distribution system. The performance of online monitoring depends highly on the quality of load data and distributed generator (DG) outputs. Accurate DG outputs and load data may also help detect errors in switch status and control device settings. In practice, direct measurements are only available at distribution substations, transformers and some important loads. Hence, estimation of DG outputs and load in power distribution systems is challenging as a large number of loads and DG outputs should be estimated with limited synchronized measurements (Naka *et al.*, 2003; Baran *et al.*, 2005; Niknam *et al.*, 2005a). Hence, there is a need for proper problem formulations and solution algorithms.

State estimators have been developed to provide the necessary data for real-time control of transmission networks, typically based on the weighted least squares approach, which determines the system states

by minimizing the mean square error of a determined set of equations. A number of distribution state estimation (DSE) methods have been developed. Naka *et al.*(2003) presented a hybrid particle swarm optimization for practical distribution state estimation, considering nonlinear characteristics of the practical equipment and actual limited measurements in distribution systems. Niknam *et al.*(2005a) presented an approach based on ant colony optimization (ACO) for DSE of a distribution system including DGs, where the values of loads and DGs are considered as state variables. Baran *et al.*(2005) presented a regression-based model and made use of the strong correlation between the loads that are geographically close to each other to address the load estimation problem. Wang and Schulz (2004) presented a branch-current-based three-phase state estimation algorithm for distribution systems, where the magnitude and phase angle of the branch current are chosen as the state variables. Gursoy and Niebur (2006) presented estimation of electric load profiles using an online independent component analysis (ICA) algorithm with an

adaptive learning parameter. A system for estimating load curves at low-voltage substations has been described by Konjic *et al.* (2005). The system is built by the aggregation of individual fuzzy inference systems of the Takagi-Sugeno type. The model is developed from actual measurements forming a base of raw data of consumer behaviors. The load estimation problem in unbalanced, radial power-distribution networks has been modeled by Wan and Miu (2002) as a weighted infinity norm ( $H_\infty$ ) estimation problem with equality and inequality constraints. Deng *et al.* (2002) proposed a branch-based state estimation method for radial distribution systems that can handle most kinds of real-time measurements. In the algorithm, the weighted least squares (WLS) problem of a whole system has been decomposed into a series of WLS sub-problems and each sub-problem deals with only single branch state estimation. Ghosh *et al.* (1997) presented an approach to distribution circuit state estimation using a probabilistic extension of the radial load flow algorithm. Leou and Lu (1996) proposed a method that uses uncertain network data, load distribution information, and telemetric data for feeder voltage profile calculation, where data involved in the calculation are represented by fuzzy numbers. Sakis Meliopoulos and Zhang (1996) formulated a multi-phase power flow model, in conjunction with synchronized measurements, for state estimation of distribution systems based on fully asymmetric modeling. Roytelman and Shahidehpour (1993) presented a method for state distribution of electric power distribution in quasi real-time conditions. Baran and Kelley (1994) developed a three-phase state estimation method to increase the accuracy of load data based on the weighted least squares approach, and used a three-phase node voltage formulation.

The DSE problem is modeled as a mixed integer nonlinear programming problem because of the existence of such equipments as static var compensators (SVCs), DGs, load tap changers, and voltage regulators (VRs). Conventional and classical methods such as linear programming, mixed integer programming, quadratic programming, etc., can be used to solve this problem. However, these methods reach local minima, depending on the initial conditions and some of them cannot handle the integer problems. To solve such a problem, evolutionary methods and expert systems such as neural networks (NNs), genetic algorithms (GAs), can be utilized. But some evolutionary

methods neither reach global minima nor have short convergence time (Naka *et al.*, 2003; Niknam *et al.*, 2005a).

Recently, a new optimization algorithm based on honey-bee mating, first proposed by Afshar *et al.* (2007), has been used to solve difficult optimization problems such as optimal reservoir operation (Haddad *et al.*, 2006; Afshar *et al.*, 2007) and clustering (Fathian *et al.*, 2007).

In this paper, a new approach based on HBMO is presented for practical DSE of a power system including DGs, SVC and VRs. In this method, DGs and loads that do not have constant output are considered as the state variables, in which the differences between measured and calculated values are assumed as the objective function.

The rest of the paper is organized as follows. In Section 2, the DSE problem is formulated. In Section 3, a DG modeling is presented. The HBMO is introduced in Section 4. Application of the proposed approach to DSE is shown in Section 5. Finally, in Section 6, the feasibility of the proposed approach is demonstrated by comparison with the methods based on NNs, ACO and GA for two test systems.

## DISTRIBUTION STATE ESTIMATION INCLUDING DISTRIBUTED GENERATORS

From a mathematical point of view, the DSE problem is an optimization problem with equality and inequality constraints. The objective function is the summation of difference between the measured and calculated values. DSE of a power system including DGs can be expressed as follows.

### Objective function

The objective function is

$$\min f(\bar{X}) = \sum_{i=1}^m \omega_i (z_i - h_i(\bar{X}))^2, \quad (1)$$

where

$$\bar{X} = [\bar{P}_G, \bar{P}_L], \quad \bar{P}_G = [P_G^1, P_G^2, \dots, P_G^{N_G}], \\ \bar{P}_L = [P_L^1, P_L^2, \dots, P_L^{N_L}],$$

$\bar{X}$  is the state variable vector including the loads and DGs' outputs;  $z_i$  is the measured value;  $\omega_i$  is the

weighting factor of the  $i$ th measured variable;  $h_i$  is the state equation of the  $i$ th measured variable;  $m$  is the number of measurements;  $N_G$  and  $N_L$  are the number of DGs and loads with variable outputs, respectively;  $P_G^i$  and  $P_L^i$  are the active power of the  $i$ th DG and  $i$ th load, respectively.

### Constraints

Constraints of the objective function are defined as follows.

(1) Active power constraints of DGs:

$$P_{G,\min}^i \leq P_G^i \leq P_{G,\max}^i, \quad i = 1, 2, \dots, N_G, \quad (2)$$

where  $P_{G,\max}^i$  and  $P_{G,\min}^i$  are the maximum and minimum active power of the  $i$ th DG, respectively.

(2) Distribution line limits:

$$\left| P_{ij}^{\text{Line}} \right| < P_{ij,\max}^{\text{Line}}, \quad (3)$$

where  $\left| P_{ij}^{\text{Line}} \right|$  and  $P_{ij,\max}^{\text{Line}}$  are the absolute power flowing over distribution lines and maximum transmission power between nodes  $i$  and  $j$ , respectively.

(3) Tap of transformers:

$$T_i^{\min} < T_i < T_i^{\max}, \quad i = 1, 2, \dots, N_t, \quad (4)$$

where  $T_i^{\min}$ ,  $T_i^{\max}$  and  $T_i$  are the minimum, maximum and current tap positions of the  $i$ th transformer, respectively;  $N_t$  is the number of transformers and VRs installed along the feeder.

(4) Bus voltage magnitude:

$$V_{\min} \leq V_i \leq V_{\max}, \quad i = 1, 2, \dots, N_b, \quad (5)$$

where  $V_i$ ,  $V_{\max}$  and  $V_{\min}$  are the actual voltage magnitude of the  $i$ th bus, the maximum and minimum values of the voltage magnitudes, respectively;  $N_b$  is the number of buses.

(5) Active power constraints of loads:

$$P_{L,\min}^i \leq P_L^i \leq P_{L,\max}^i, \quad i = 1, 2, \dots, N_L, \quad (6)$$

where  $P_{L,\min}^i$  and  $P_{L,\max}^i$  are the minimum and maximum active power of the  $i$ th load, respectively.

(6) Reactive power constraints of capacitors:

$$0 \leq Q_c^i \leq Q_{c,\max}^i, \quad i = 1, 2, \dots, N_c, \quad (7)$$

where  $Q_c^i$  and  $Q_{c,\max}^i$  are the reactive power and maximum reactive power of the  $i$ th capacitor, respectively;  $N_c$  is the number of capacitors installed along the feeder.

(7) Unbalanced three-phase power flow equations.

It is assumed in this study that capacitors and VRs, which change stepwise and are installed along feeders, are locally controlled. During the search procedure, change of state variables (loads and DGs' outputs) may cause change of tap positions and capacitor banks, which consequently makes the objective function change discontinuously.

The number of measurements in distribution systems is usually less than that of the state variables. In order to have a unique solution, we make the following assumptions:

- Statuses of distribution lines and switches are known;
- A contracted load and distributed generation values are known at each node;
- Voltage and current at the substation bus (main bus) are known;
- If outputs of DGs and loads are fixed, the outputs and power factors are available;
- If outputs of DGs and loads are variable, the average outputs, the standard deviations, and the power factors can be obtained;
- Set points of VRs and local capacitors are known.

In this study the average and standard deviation values of DGs and loads, which are variable, are considered as the pseudo measurement devices. In Eq.(1),  $\omega_i$  should be considered high for real instrument devices and low for pseudo instrument devices. In this research these values are 10 and 0.1, respectively.

### DISTRIBUTED GENERATION MODELING

DGs are the electric energy resources connected to the distribution network. Since DGs are closely connected to the loads, they can increase the power quality and reliability from the customers' perspective

and help the utilities to face the load growth by delaying the upgrade of distribution/transmission lines. In addition to that, small generating systems require limited capital investments and reduced authorizations to be installed. Also, DGs using renewable energies are often encouraged and financially supported thanks to their low environmental impact (Niknam, 2005; Niknam *et al.*, 2005b; Losi and Russo, 2005).

Generally, DGs in distribution load flow can be modeled as a PV or a PQ model. Since distribution networks are unbalanced three-phase systems, DGs can be controlled and operated in two forms: (1) simultaneous three-phase control, and (2) independent three-phase control or single-phase control. Therefore, with regard to the control methods and DGs models, four models can be defined for the simulation of these generators, as shown in Fig.1.

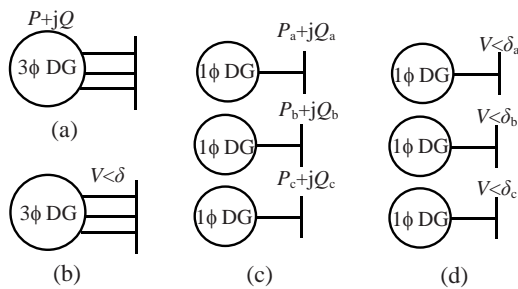


**Fig.1 Four models of distributed generators. (a) PQ model with simultaneous three-phase control; (b) PV model with simultaneous three-phase control; (c) PQ model with independent three-phase control; (d) PV model with independent three-phase control**

When DGs are considered as the PV models, they have to be able to generate reactive power to maintain their voltage magnitudes. Several procedures have been presented to model DGs as the PV buses (Niknam, 2005; Niknam *et al.*, 2005b; Losi and Russo, 2005). Fig.1 shows the model of DGs based on their control type. In this study, DGs are modeled as the PQ model with simultaneous three-phase control (Fig.1a).

### HONEY-BEE MODELING

The honey bee is a social insect that can survive only as a member of a community, or colony. The colony inhabits an enclosed cavity. The honey-bee community consists of three structurally different forms—the queen (reproductive female), the drone (male), and the worker (no reproductive female). These castes are associated with different functions in the colony; each caste possesses its own special instincts geared to the needs of the colony. The HBMO algorithm combines a number of different procedures. Each of them corresponds to a different phase of the mating process of the honey-bee that is presented in Fig.2 (Afshar *et al.*, 2007).

A drone mates with a queen probabilistically using an annealing function as follows (Haddad *et al.*, 2006):

$$Prob(D)=\exp(-\Delta(f)/S(t)), \quad (8)$$

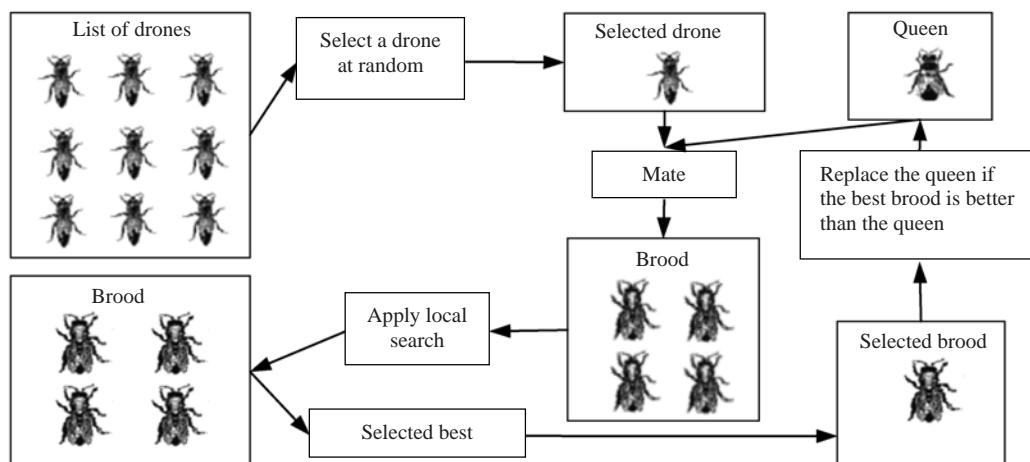


**Fig.2 Honey-bee mating optimization algorithm (Afshar *et al.*, 2007)**

where  $Prob(D)$  is the probability of adding the sperm of drone  $D$  to the spermatheca of the queen (that is, the probability of a successful mating),  $\Delta(f)$  is the absolute difference between the fitness of  $D$  and the fitness of the queen (for complete description of the calculation of the fitness function, see below), and  $S(t)$  is the speed of the queen at time  $t$ . The probability of mating is high when the queen is with the high speed level, or when the fitness of the drone is as good as the queen's. After each transition in space, the queen's speed and energy decrease according to the following equations:

$$S(t+1)=\alpha \cdot S(t), \quad (9)$$

$$En(t+1)=\alpha \cdot En(t), \quad (10)$$

where  $\alpha \in (0, 1)$  is the amount of speed and energy reduction after each transition and each step. Initially, the speed and energy of the queen are generated at random. The speed and energy have the same effect, and one of them should be used. In this study the speed of the queen is considered. A number of mating flights are realized. At the start of a mating flight drones are generated randomly and the queen selects a drone using the probabilistic rule in Eq.(8). If the mating is successful (i.e., the drone passes the probabilistic decision rule), the drone's sperm is stored in the queen's spermatheca. By using the crossover of the drone and the queen's genotypes, a new brood (trial solution) is generated, which can be improved later by employing workers to conduct a local search. One of the major differences between the HBMO algorithm and the classic evolutionary algorithms is that since the queen stores many drones' sperm in her spermatheca, she can utilize parts of the genotype of different drones to create a new solution which gives the possibility to have the fittest broods more. In real life, the role of the workers is restricted to brood care and for this reason the workers are not separate members of the population and they are used as local search procedures in order to improve the broods produced by the mating flight of the queen. Each of the workers has different capabilities and the choices of two different workers may produce different solutions. This is realized with the use of a number of single local search heuristics ( $N_{W1}$ ) and combinations of them ( $N_{W2}$ ). Thus, the sum of these two numbers ( $N_W=N_{W1}+N_{W2}$ ) gives the number of workers. Each

of the broods is randomly chosen to be fed by the worker, which is also randomly selected. If the new brood is better than the current queen, it takes the place of the queen. If the brood fails to replace the queen, in the next mating flight this brood will be one of the drones.

## APPLICATION OF HBMO TO DSE

This section presents the application of the proposed algorithm for solving the DSE problem. It should be noted that the state variables are values of the loads and DGs whose outputs are variable, rather than voltage or current as used by conventional state estimations. To apply the HBMO, the following steps have to be taken.

Step 1: Define the input data.

In this step, the input data are defined, including the distribution line status, the real and pseudo measured values, DGs and loads status, the average and standard deviation of loads and DGs, the speed of the queen at the start of a mating flight ( $S_{max}$ ), the speed of the queen at the end of a mating flight ( $S_{min}$ ), the speed reduction schema ( $\alpha$ ), the number of iterations, the number of workers ( $N_W$ ), the number of drones ( $N_D$ ), the size of the queen's spermatheca ( $N_S$ ) and the number of broods ( $N_B$ ).

Step 2: Transfer the constrained DSE to the unconstrained DSE.

The proposed DSE problem needs to be transformed into an unconstrained one by constructing an augmented objective function incorporating penalty factors for any value violating the constraints.

$$F(\bar{X}) = f(\bar{X}) + k_1 \sum_{j=1}^{N_{eq}} (J_j(\bar{X}_j))^2 + k_2 \sum_{l=1}^{N_{ueq}} (\max(0, -g_l(\bar{X}_l)))^2, \\ J_j(\bar{X}) = 0, j=1, 2, \dots, N_{eq}; g_l(\bar{X}) > 0, l=1, 2, \dots, N_{ueq}, \quad (11)$$

where  $f(\bar{X})$  is the objective function value of the DSE problem;  $N_{eq}$  and  $N_{ueq}$  are the number of equality and inequality constraints, respectively;  $J_j(\bar{X}_j)$  and  $g_l(\bar{X}_l)$  are the equality and inequality constraints, respectively;  $k_1$  and  $k_2$  are the penalty factors. Since the constraints should be met,  $k_1$  and  $k_2$  should be high. In this study  $k_1=k_2=100000$ .

In the DSE problem, the augmented objective function is calculated as follows. At first, the distribution load flow runs based on the state variables (values of loads and DGs). Based on the results of the distribution load flow,  $f(\bar{X})$  is calculated and the constraints are checked. Then the augmented objective function is calculated using the values of the objective function and constraints.

Step 3: Generate the initial population  $P_{ini}$ .

In this step, an initial population based on state variables is generated randomly, formulated as

$$P_{ini} = \begin{bmatrix} \bar{X}_1 \\ \bar{X}_2 \\ \vdots \\ \bar{X}_N \end{bmatrix}, \quad (12)$$

where

$\bar{X}_i = (x_j)_{1 \times n} = [P_{G,i}^1, P_{G,i}^2, \dots, P_{G,i}^{N_G}, P_{L,i}^1, P_{L,i}^2, \dots, P_{L,i}^{N_L}]$ ,  $i=1, 2, \dots, N$ ;  $P_{G,\min}^j \leq P_{G,i}^j \leq P_{G,\max}^j$ ,  $j=1, 2, \dots, N_G$ ;  $P_{L,\min}^k \leq P_{L,i}^k \leq P_{L,\max}^k$ ,  $k=1, 2, \dots, N_L$ ;  $n = N_G + N_L$ .  $x_j$  is the  $j$ th state variable,  $n$  is the number of state variables, and  $N$  is the number of members in the initial population.

Step 4: Calculate the augmented objective function value.

In this step, the augmented objective function, Eq.(11), is to be evaluated for each individual by using the result of the distribution load flow.

Step 5: Sort the initial population based on the objective function values.

The initial population is ascending based on the value of the objective function.

Step 6: Select the queen.

The individual that has the minimum objective function ( $\bar{X}_{best}$ ) should be selected as the queen.

Step 7: Generate the queen speed  $S_{queen}$ .

The queen speed is randomly generated as

$$S_{queen} = \text{rand}(\cdot)(S_{\max} - S_{\min}) + S_{\min}, \quad (13)$$

where  $\text{rand}(\cdot)$  is a random function generator.

Step 8: Select the population of drones  $P_D$ .

The population of drones is selected from the sorted initial population as

$$P_D = \begin{bmatrix} D_1 \\ D_2 \\ \vdots \\ D_{N_D} \end{bmatrix}, \quad (14)$$

where  $D_i = [P_{G,i}^1, P_{G,i}^2, \dots, P_{G,i}^{N_G}, P_{L,i}^1, P_{L,i}^2, \dots, P_{L,i}^{N_L}]$ ,  $i=1, 2, \dots, N_D$ .  $D_i$  refers to the  $i$ th drone.

Step 9: Generate the queen's spermatheca matrix (mating flight)  $S_p$ .

At the start of the mating flight, the queen flies with her maximum speed. A drone is randomly selected from the population of drones. The mating probability is calculated based on the objective function values of the queen and the selected drones. A number between 0 and 1 is randomly generated and compared with the calculated probability. If it is less than the calculated probability, the drone's sperm is sorted in the queen's spermatheca and the queen speed decreases. Otherwise, the queen speed decreases and another drone from the population of drones is selected until the speed of the queen reaches her minimum speed or the queen's spermatheca is full.

$$S_p = \begin{bmatrix} S_1 \\ S_2 \\ \vdots \\ S_{N_S} \end{bmatrix}, \quad (15)$$

where  $S_i = (s_j)_{1 \times n} = [P_{G,i}^1, P_{G,i}^2, \dots, P_{G,i}^{N_G}, P_{L,i}^1, P_{L,i}^2, \dots, P_{L,i}^{N_L}]$ ,  $i=1, 2, \dots, N_S$ .  $S_i$  represents the  $i$ th individual in the queen's spermatheca.

Step 10: Breeding process.

In this step, a population of broods is generated based on the mating between the queen and the drones stored in the queen's spermatheca. The  $j$ th brood is generated using the following process:

$$\begin{cases} \bar{X}_{best} = [x_{best}^1, x_{best}^2, \dots, x_{best}^n], \\ S_i = [s_i^1, s_i^2, \dots, s_i^n], \\ B_j = \bar{X}_{best} + \beta(\bar{X}_{best} - S_i), j = 1, 2, \dots, N_B, \end{cases} \quad (16)$$

where  $\beta$  is a random number between 0 and 1, and  $B_j$  refers to the  $j$ th brood.

Step 11: Feeding selected broods and the queen with the royal jelly by workers.

The population of broods is improved by applying different heuristic functions and mutation operators. At first the  $i$ th brood is randomly selected. Two integral numbers ( $B_1$  and  $B_2$ ) between 1 and  $n$  are randomly generated. It is assumed  $B_1 < B_2$ . The brood is changed and improved as follows:

$$B_i(j) = \begin{cases} B_i(j), & j < B_1 \text{ or } j > B_2, \\ \text{rand}(\cdot)(x_{\max}^j - x_{\min}^j) + x_{\min}^j, & B_1 \leq j \leq B_2, \end{cases} \quad (17)$$

where  $i=1, 2, \dots, N_W$ ,  $x_{\max}^j$  and  $x_{\min}^j$  are the maximum and minimum values of the  $j$ th state variable, respectively.

Step 12: Calculate the augmented objective function value for the newly generated solutions.

The augmented objective function, Eq.(11), is to be evaluated for each individual of the newly generated solutions by using the result of the distribution load flow. If the new best solution is better than the queen, replace the queen with the new best solution.

Step 13: Check the termination criteria.

If the termination criteria are satisfied, end; else, discard all previous trial solutions and go to Step 3 until the convergence criteria are met.

### SIMULATION RESULTS

In this section, the proposed method is applied to DSE of two distribution test systems. It is assumed that the following information is available:

- (1) Value of output for constant loads and DGs;
- (2) Average value and standard deviation for variable DGs and loads;
- (3) Values of measured points;
- (4) Power factor of loads and DGs;
- (5) Set points of VRs and local capacitors.

In the following, results for two cases—IEEE 34-bus radial test feeders and a realistic 80-bus 20 kV network—are presented.

#### IEEE 34-bus radial test feeders

Fig.3 shows the IEEE 34-bus radial distribution test feeders, whose associated specifications are presented in (Kersting, 1991).

For this system it is assumed that there are three DGs connected to buses 6, 17 and 29, respectively, whose specifications are presented in Table 1. There are also eight variable loads, whose specifications are demonstrated in Table 2.

**Table 1 Characteristics of the three generators**

| Parameter                           | G1  | G2  | G3  |
|-------------------------------------|-----|-----|-----|
| Average of active power output (kW) | 60  | 80  | 90  |
| Standard deviation (%)              | 25  | 15  | 15  |
| Power factor                        | 0.8 | 0.8 | 0.8 |

**Table 2 Characteristics of variable loads**

| Location | Active power (kW) |     |     | Reactive power (kV·A) |      |     | Standard deviation (%) |
|----------|-------------------|-----|-----|-----------------------|------|-----|------------------------|
|          | a                 | b   | c   | a                     | b    | c   |                        |
| Bus 2    | 0                 | 32  | 26  | 0                     | 16.5 | 14  | 20                     |
| Bus 10   | 34                | 0   | 0   | 18                    | 0    | 0   | 15                     |
| Bus 12   | 136               | 0   | 0   | 70                    | 0    | 0   | 15                     |
| Bus 13   | 0                 | 42  | 0   | 0                     | 22   | 0   | 10                     |
| Bus 22   | 27                | 27  | 27  | 22                    | 22   | 22  | 20                     |
| Bus 27   | 134               | 134 | 134 | 107                   | 107  | 107 | 10                     |
| Bus 29   | 20                | 20  | 131 | 16                    | 16   | 73  | 15                     |
| Bus 30   | 20                | 20  | 62  | 16                    | 16   | 38  | 20                     |

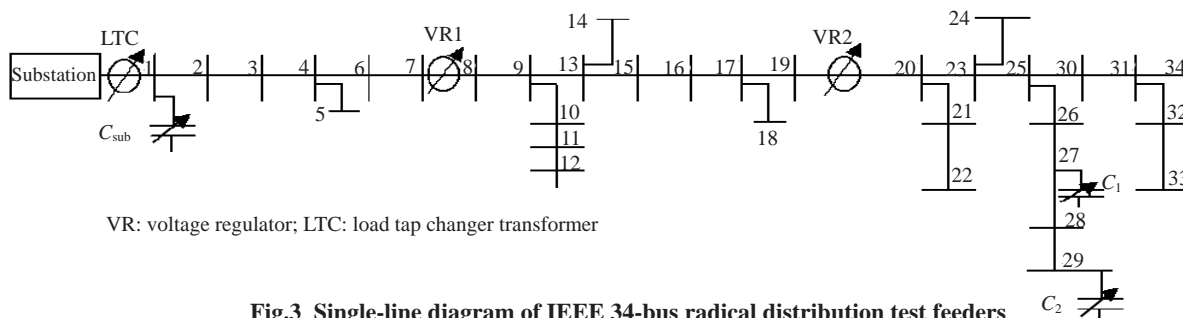


**Fig.3 Single-line diagram of IEEE 34-bus radial distribution test feeders**

It is assumed that there are three measurement devices installed on buses 1, 15 and 25, respectively. The values of these devices are obtained using the results of the distribution load flow.

There are several parameters to be determined for implementation of the HBMO algorithm. Simulation was carried out to find the best value of each parameter. The results are shown in Table 3.

One hundred random trails were performed for each parameter set. The best values for these parameters are selected as follows:  $S_{max}=1$ ,  $S_{min}=0.2$ ,  $\alpha=0.93$ ,  $N_D=20$ ,  $N_W=N_S=N_B=15$ .

Tables 4~8 show the simulation results of ACO, GA, NN, and the proposed method for estimation of loads and DGs values, respectively.

**Table 3 Ranges of algorithmic parameters**

| Parameter | Maximum limit | Minimum limit | Step size |
|-----------|---------------|---------------|-----------|
| $S_{max}$ | 1.5           | 1.0           | -0.10     |
| $S_{min}$ | 0.2           | 0             | -0.01     |
| $\alpha$  | 1             | 0.8           | -0.01     |
| $N_W$     | 20            | 1             | 1         |
| $N_D$     | 30            | 1             | 1         |
| $N_S$     | 20            | 1             | 1         |
| $N_B$     | 20            | 1             | 1         |

$S_{max}$ ,  $S_{min}$ : speeds of the queen at the start and the end of a mating flight, respectively;  $\alpha$ : speed reduction schema;  $N_W$ ,  $N_D$ ,  $N_S$ ,  $N_B$ : numbers of workers, drones, queen's spermatheca, broods, respectively

**Table 4 Simulation results of ACO for the actual and estimated values of loads at different locations (active power: kW; reactive power: kV·A)\***

| Phase | Power type | Value type | Bus 2 | Bus 10 | Bus 12 | Bus 13 | Bus 22 | Bus 27 | Bus 29      | Bus 30 |
|-------|------------|------------|-------|--------|--------|--------|--------|--------|-------------|--------|
| a     | Active     | Actual     | 0     | 35     | 140    | 0      | 28     | 140    | 21          | 21     |
|       |            | Estimated  | 0     | 35.2   | 141.3  | 0      | 27.8   | 140.8  | 20.7        | 21.0   |
|       | Reactive   | Actual     | 0     | 18.5   | 74     | 0      | 23     | 113    | 17          | 17     |
|       |            | Estimated  | 0     | 18.9   | 72.9   | 0      | 22.8   | 112.9  | 17.2        | 16.8   |
| b     | Active     | Actual     | 33    | 0      | 0      | 44     | 28     | 140    | 21          | 21     |
|       |            | Estimated  | 33.2  | 0      | 0      | 43.6   | 28.8   | 140.8  | 21.6        | 20.9   |
|       | Reactive   | Actual     | 17    | 0      | 0      | 23     | 23     | 113    | 17          | 17     |
|       |            | Estimated  | 16.3  | 0      | 0      | 22.4   | 23.8   | 112.2  | 16.9        | 17.8   |
| c     | Active     | Actual     | 28    | 0      | 0      | 0      | 28     | 140    | 137         | 65     |
|       |            | Estimated  | 27.6  | 0      | 0      | 0      | 28.4   | 141.3  | 136.9       | 63.4   |
|       | Reactive   | Actual     | 15    | 0      | 0      | 0      | 23     | 113    | 77          | 40     |
|       |            | Estimated  | 14.3  | 0      | 0      | 0      | 22.7   | 112.4  | <b>78.7</b> | 38.5   |

\* Data come from (Niknam, 2005; Niknam *et al.*, 2005a; 2005b). Simulation conditions are: number of colonies=30; number of ants in each colony=10; evaporation rate  $\rho=0.9$ ; control parameters for determining the weight of trail intensity ( $\gamma_1$ ) and length of path ( $\gamma_2$ ):  $\gamma_1=4$ ,  $\gamma_2=2$

**Table 5 Simulation results of GA for the actual and estimated values of loads at different locations (active power: kW; reactive power: kV·A)\***

| Phase | Power type | Value type | Bus 2 | Bus 10 | Bus 12 | Bus 13 | Bus 22 | Bus 27 | Bus 29 | Bus 30      |
|-------|------------|------------|-------|--------|--------|--------|--------|--------|--------|-------------|
| a     | Active     | Actual     | 0     | 35     | 140    | 0      | 28     | 140    | 21     | 21          |
|       |            | Estimated  | 0     | 36.2   | 140.1  | 0      | 27.8   | 140.1  | 20.6   | 20.1        |
|       | Reactive   | Actual     | 0     | 18.5   | 74     | 0      | 23     | 113    | 17     | 17          |
|       |            | Estimated  | 0     | 18.2   | 73.5   | 0      | 22.3   | 112.1  | 16.1   | 16.8        |
| b     | Active     | Actual     | 33    | 0      | 0      | 44     | 28     | 140    | 21     | 21          |
|       |            | Estimated  | 33.8  | 0      | 0      | 45.6   | 27.8   | 140.6  | 20.7   | 21.9        |
|       | Reactive   | Actual     | 17    | 0      | 0      | 23     | 23     | 113    | 17     | 17          |
|       |            | Estimated  | 17.6  | 0      | 0      | 22.6   | 23.2   | 113.8  | 16.4   | 17.0        |
| c     | Active     | Actual     | 28    | 0      | 0      | 0      | 28     | 140    | 137    | 65          |
|       |            | Estimated  | 27.4  | 0      | 0      | 0      | 28.4   | 140.1  | 137.1  | 65.1        |
|       | Reactive   | Actual     | 15    | 0      | 0      | 0      | 23     | 113    | 77     | 40          |
|       |            | Estimated  | 14.2  | 0      | 0      | 0      | 23.5   | 112.9  | 76.2   | <b>38.2</b> |

\* Data come from (Niknam, 2005; Niknam *et al.*, 2005a; 2005b). Integer strings instead of binary coding are used to represent value of variables, and include the following processes (Haupt and Haupt, 1999): representation and initialization, fitness function, reproduction operation, crossover operation, and mutation operation. Simulation conditions are: initial population=1 000; selected population=100; mutation=4%; crossover probability=0.7-0.8



**Table 6 Simulation results of NN for the actual and estimated values of loads at different locations (active power: kW; reactive power: kV·A)\***

| Phase | Power type | Value type | Bus 2 | Bus 10 | Bus 12       | Bus 13 | Bus 22 | Bus 27 | Bus 29 | Bus 30 |
|-------|------------|------------|-------|--------|--------------|--------|--------|--------|--------|--------|
| a     | Active     | Actual     | 0     | 35     | 140          | 0      | 28     | 140    | 21     | 21     |
|       |            | Estimated  | 0     | 35.0   | <b>144.3</b> | 0      | 28.0   | 140.9  | 20.0   | 21.2   |
|       | Reactive   | Actual     | 0     | 18.5   | 74           | 0      | 23     | 113    | 17     | 17     |
|       |            | Estimated  | 0     | 19.0   | 74.2         | 0      | 22.6   | 112.9  | 16.5   | 16.7   |
| b     | Active     | Actual     | 33    | 0      | 0            | 44     | 28     | 140    | 21     | 21     |
|       |            | Estimated  | 31.5  | 0      | 0            | 45.7   | 27.9   | 141.9  | 20.1   | 22.1   |
|       | Reactive   | Actual     | 17    | 0      | 0            | 23     | 23     | 113    | 17     | 17     |
|       |            | Estimated  | 16.7  | 0      | 0            | 22.8   | 22.6   | 112.3  | 16.7   | 17.7   |
| c     | Active     | Actual     | 28    | 0      | 0            | 0      | 28     | 140    | 137    | 65     |
|       |            | Estimated  | 29.0  | 0      | 0            | 0      | 27.3   | 140.9  | 135.4  | 63.2   |
|       | Reactive   | Actual     | 15    | 0      | 0            | 0      | 23     | 113    | 77     | 40     |
|       |            | Estimated  | 14.2  | 0      | 0            | 0      | 22.1   | 114.3  | 76.3   | 38.3   |

\* Data come from (Niknam, 2005; Niknam *et al.*, 2005a; 2005b). Simulation conditions are: number of total patterns=2 000; number of training patterns=1 500; test data=500; number of hidden layers=1; number of neurons in hidden layers=4; number of neurons in input layers=number of measurement devices; number of neurons in output layers=number of DGs+number of loads

**Table 7 Simulation results of HBMO for the actual and estimated values of loads at different locations (active power: kW; reactive power: kV·A)\***

| Phase | Power type | Value type | Bus 2 | Bus 10 | Bus 12      | Bus 13 | Bus 22 | Bus 27 | Bus 29 | Bus 30 |
|-------|------------|------------|-------|--------|-------------|--------|--------|--------|--------|--------|
| a     | Active     | Actual     | 0     | 35     | 140         | 0      | 28     | 140    | 21     | 21     |
|       |            | Estimated  | 0     | 35.1   | 39.3        | 0      | 28.2   | 140.4  | 20.6   | 21.1   |
|       | Reactive   | Actual     | 0     | 18.5   | 74          | 0      | 23     | 113    | 17     | 17     |
|       |            | Estimated  | 0     | 18.1   | <b>75.2</b> | 0      | 22.6   | 112.2  | 17.1   | 17.2   |
| b     | Active     | Actual     | 33    | 0      | 0           | 44     | 28     | 140    | 21     | 21     |
|       |            | Estimated  | 33.0  | 0      | 0           | 43.24  | 28.3   | 139.8  | 20.1   | 21.3   |
|       | Reactive   | Actual     | 17    | 0      | 0           | 23     | 23     | 113    | 17     | 17     |
|       |            | Estimated  | 16.6  | 0      | 0           | 23.55  | 23.4   | 113.2  | 17.0   | 17.2   |
| c     | Active     | Actual     | 28    | 0      | 0           | 0      | 28     | 140    | 137    | 65     |
|       |            | Estimated  | 27.7  | 0      | 0           | 0      | 27.5   | 139.1  | 138.6  | 65.1   |
|       | Reactive   | Actual     | 15    | 0      | 0           | 0      | 23     | 113    | 77     | 40     |
|       |            | Estimated  | 14.8  | 0      | 0           | 0      | 22.7   | 114.6  | 77.3   | 41.2   |

**Table 8 Comparison of the actual and estimated values of DGs**

| DG | HBMO   |             | ACO    |             | GA     |             | NN     |             |
|----|--------|-------------|--------|-------------|--------|-------------|--------|-------------|
|    | Actual | Estimated   | Actual | Estimated   | Actual | Estimated   | Actual | Estimated   |
| G1 | 56     | <b>57.1</b> | 56     | 56.3        | 56     | 57.4        | 56     | 58.2        |
| G2 | 85     | 84.2        | 85     | <b>86.9</b> | 85     | 83.4        | 85     | 84.2        |
| G3 | 85     | 85.6        | 85     | 86.3        | 85     | <b>87.7</b> | 85     | <b>87.6</b> |

According to Tables 4~8, the maximum error of HBMO between the values of the estimated and actual loads is 1.2, while for the ACO, GA and NN they are 1.7, 1.8 and 4.3, respectively. The maximum errors of HBMO, ACO, GA and NN for estimation of DG outputs are 1.1, 1.9, 2.7 and 2.6, respectively. The simulation results show that the accuracy of the proposed algorithm is better than those of other algorithms.

Table 9 shows the execution time and average

and standard deviation for different runs of these algorithms. The execution time of the NN algorithm is less than that of the proposed method, while the proposed method is more feasible than NN. The reason is that NN results need too many training patterns, but the proposed algorithm requires only network data and measured values. The execution time of the proposed method changes between 15 s and 20 s, which is less than that obtained by other evolutionary algorithms.

**Table 9 Comparison of execution time, average, and standard deviation for different runs**

| Method | Execution time (s) | Average ( $\times 10^{-3}$ ) | Standard deviation (%) |
|--------|--------------------|------------------------------|------------------------|
| ACO    | 20~40              | 0.20                         | 10                     |
| GA     | 100~120            | 0.30                         | 12                     |
| NN     | ~0                 | 1.20                         | 0                      |
| HBMO   | 15~20              | 0.18                         | 8                      |

As shown in Table 9, the average evaluation value of the proposed algorithm for different runs is  $0.18 \times 10^{-3}$ , which is approximately 90%, 60% and 15% of that obtained by ACO, GA and NN, respectively. The standard deviation of NN is zero, which is less than that of other algorithms, but the results of NN depend on the number of training patterns. These results indicate that the quality of the solutions obtained by HBMO is higher than that of others.

Tables 10 and 11 show the simulation results for the following errors.

Maximum individual relative error:

$$MIRE (\%) = \max \left( \left| \frac{X_{est}(i) - X_{true}(i)}{X_{true}(i)} \right| \right) \times 100. \quad (18)$$

Maximum individual absolute error:

$$MIAE = \max \left( \left| X_{est}(i) - X_{true}(i) \right| \right). \quad (19)$$

In Eqs.(18) and (19),  $X_{est}(i)$  and  $X_{true}(i)$  are the estimated and actual values of the  $i$ th bus, respectively.

**Table 10 Maximum individual relative and absolute errors for estimated loads and the bus where the error occurs**

| Method | Relative error  |          | Absolute error |          |
|--------|-----------------|----------|----------------|----------|
|        | <i>MIRE</i> (%) | Location | <i>MIAE</i>    | Location |
| ACO    | 4.88            | 30       | 1.67           | 29       |
| HBMO   | 4.10            | 29       | 1.24           | 12       |
| NN     | 5.13            | 2        | 4.31           | 12       |
| GA     | 5.33            | 2        | 1.77           | 30       |

**Table 11 Maximum individual relative and absolute errors for estimated DGs**

| Method | Relative error  |          | Absolute error |          |
|--------|-----------------|----------|----------------|----------|
|        | <i>MIRE</i> (%) | Location | <i>MIAE</i>    | Location |
| ACO    | 2.24            | DG2      | 1.90           | DG2      |
| HBMO   | 1.96            | DG1      | 1.10           | DG1      |
| NN     | 3.93            | DG1      | 2.64           | DG3      |
| GA     | 3.14            | DG3      | 2.67           | DG3      |

According to the results of Tables 10 and 11, the mentioned errors of the HBMO algorithm for estimation of loads are 4.10% and 1.24, respectively, which are the minima. The errors of the HBMO algorithm for estimation of DGs are 1.96% and 1.10, respectively. The results show that the HBMO algorithm can generate higher quality solutions compared with ACO, GA and NN algorithms.

### A realistic 80-bus 20 kV network

Fig.4 shows the single-line diagram of a realistic 80-bus 20 kV network used to supply power demand in an urban area located in the Fars Province, Iran (Niknam *et al.*, 2005b). As there is no DG in this network currently, it is assumed that there are six DGs, whose specifications are given in Table 12. Also there are 10 variable loads whose specifications are demonstrated in Table 13. The network is symmetrical.

**Table 12 Characteristics of generators**

| Parameter                           | G1  | G2  | G3  | G4  | G5  | G6  |
|-------------------------------------|-----|-----|-----|-----|-----|-----|
| Average of active power output (kW) | 60  | 80  | 90  | 120 | 200 | 150 |
| Standard deviation (%)              | 25  | 15  | 15  | 15  | 15  | 15  |
| Power factor                        | 0.8 | 0.8 | 0.8 | 0.8 | 0.8 | 0.8 |
| Actual value (kW)                   | 50  | 75  | 85  | 125 | 210 | 140 |

**Table 13 Characteristics of variable loads**

| Location                 | Active power output (kW) |              | Reactive power output (kV·A) |              | Standard deviation (%) |
|--------------------------|--------------------------|--------------|------------------------------|--------------|------------------------|
|                          | Average                  | Actual value | Average                      | Actual value |                        |
| Buses 2, 25, 28, 30      | 200                      | 210          | 110                          | 105          | 10                     |
| Buses 43, 56, 63, 75, 78 | 150                      | 160          | 80                           | 81           | 10                     |

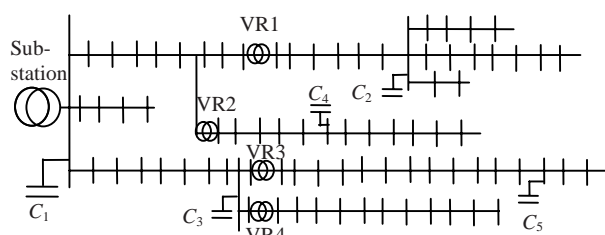


**Fig.4** Single-line diagram of a realistic 80-bus test system

The simulation results of the proposed method, ACO, GA and NN are presented in Table 14. The execution time of HBMO is between 15 s and 20 s for different runs, which is less than that of GA and ACO but more than that of NN. The standard deviation of NN is zero, as illustrated in Table 14, but the average evaluation value of NN is the worst, and the results of NN highly depend on the training patterns. The average evaluation value of HBMO is  $0.19 \times 10^{-3}$ , which is the best. These results demonstrate that the proposed algorithm converges to a global optimum with a smaller standard deviation and less execution time.

**Table 14** Comparison of execution time, average, and standard deviation for different executions

| Method | Average<br>( $\times 10^{-3}$ ) | Execution time<br>(s) | Standard<br>deviation (%) |
|--------|---------------------------------|-----------------------|---------------------------|
| ACO    | 0.40                            | 30~40                 | 10                        |
| GA     | 0.90                            | 120~130               | 13                        |
| NN     | 1.80                            | ~0                    | 0                         |
| HBMO   | 0.19                            | 15~20                 | 8                         |

## CONCLUSION

In this study, an efficient evolutionary approach based on the HBMO algorithm is introduced to estimate distribution state variables in the presence of DGs. The simulation results show that the execution time of the proposed algorithm is significantly shorter compared to GA and ACO, and give the general idea that the method can be implemented without any restriction in practical networks. The proposed algorithm requires more execution time than the NN algorithm, but it is more feasible as it requires only network data and measured values, while the NN algorithm needs too many training patterns. The proposed algorithm reaches a better optimal solution compared with other methods and has a small

standard deviation for different trials. Also, the simulation results indicate that the estimation errors are at acceptable levels. The proposed DSE can estimate the states of system when the measurement devices have errors. The proposed algorithm can estimate appropriate loads and DG outputs at each node with limited measurement points in distribution networks. The maximum individual relative error and maximum individual absolute error for the proposed method are less than those of other methods. The major deficiency with the HBMO algorithm is the tuning of its parameters, which might be different from case to case.

## References

- Afshar, A., Bozog, H., Marino, M.A., Adams, B.J., 2007. Honey-bee mating optimization (HBMO) algorithm for optimal reservoir operation. *J. Franklin Inst.*, **344**(5): 452-462. [doi:10.1016/j.jfranklin.2006.06.001]
- Baran, M.E., Kelley, A.W., 1994. State estimation for real-time monitoring of distribution systems. *IEEE Trans. on Power Syst.*, **9**(3):1601-1609. [doi:10.1109/59.336098]
- Baran, M.E., Freeman, L.A.A., Hanson, F., Ayers, V., 2005. Load estimation for load monitoring at distribution substations. *IEEE Trans. on Power Syst.*, **20**(1):164-170. [doi:10.1109/TPWRS.2004.840409]
- Deng, Y., He, Y., Zhang, B., 2002. A branch-estimation-based state estimation method for radial distribution systems. *IEEE Trans. on Power Del.*, **17**(4):1057-1062. [doi:10.1109/TPWRD.2002.803800]
- Fathian, M., Amiri, B., Maroosi, A., 2007. Application of honey bee mating optimization algorithm on clustering. *Appl. Math. Comput.*, **190**(2):1502-1513. [doi:10.1016/j.amc.2007.02.029]
- Ghosh, A.K., Lubkeman, D.L., Downey, M.J., Jones, R.H., 1997. Distribution circuit state estimation using a probabilistic approach. *IEEE Trans. on Power Syst.*, **12**(1):45-51. [doi:10.1109/59.574922]
- Gursoy, E., Niebur, D., 2006. On-line Estimation of Electric Power System Active Loads. Proc. IEEE Int. Joint Conf. on Neural Networks, BC, Canada, p.1689-1694. [doi:10.1109/IJCNN.2006.1716311]
- Haddad, O.B., Afshar, A., Marino, M.A., 2006. Honey-bees mating optimization (HBMO) algorithm: a new heuristic approach for water resources optimization. *Water Res. Manag.*, **20**(5):661-680. [doi:10.1007/s11269-005-9001-3]
- Haupt, J.R.L., Haupt, S.E., 1999. Practical Genetic Algorithm. John Wiley & Sons Inc.
- Kersting, W.H., 1991. Radial distribution test feeders. *IEEE Trans. on Power Syst.*, **6**(3):975-985. [doi:10.1109/59.119237]
- Konjic, T., Miranda, V., Kapetanovic, I., 2005. Fuzzy inference systems applied to LV substation load estimation. *IEEE Trans. on Power Syst.*, **20**(2):742-749. [doi:10.1109/TPWRS.2005.846210]

- Leou, R.C., Lu, C.N., 1996. Improving feeder voltage calculation results with telemeter data. *IEEE Trans. on Power Del.*, **11**(4):1914-1920. [doi:10.1109/61.544276]
- Losi, A., Russo, M., 2005. Dispersed generation modeling for object-oriented distribution load flow. *IEEE Trans. on Power Del.*, **20**(2):1532-1540. [doi:10.1109/TPWRD.2004.838634]
- Naka, S., Genji, T., Yura, T., Fukuyama, Y., 2003. A hybrid particle swarm optimization for distribution state estimation. *IEEE Trans. on Power Syst.*, **18**(1):60-68. [doi:10.1109/TPWRS.2002.807051]
- Niknam, T., 2005. Impact of Distributed Generators on Volt/Var Control in Distribution Networks. PhD Thesis, Electrical Engineering Department, Sharif University of Technology.
- Niknam, T., Ranjbar, A.M., Shirani, A.R., 2005a. A new approach for distribution state estimation based on ant colony algorithm with regard to distributed generation. *J. Intell. Fuzzy Syst.*, **16**(2):119-131.
- Niknam, T., Ranjbar, A.M., Shirani, A.R., 2005b. A new approach based on ant algorithm for Volt/Var control in distribution network considering distributed generation. *Iran. J. Sci. Tech., Trans. B*, **29**(B4):1-15.
- Roytelman, I., Shahidehpour, S.M., 1993. State estimation for electric power distribution systems in quasi real-time conditions. *IEEE Trans. Power Del.*, **8**(4):2009-2015. [doi:10.1109/61.248315]
- Sakis Meliopoulos, A.P., Zhang, F., 1996. Multiphase power flow and state estimation for power distribution systems. *IEEE Trans. on Power Syst.*, **11**(2):939-946. [doi:10.1109/59.496178]
- Wan, J., Miu, K.N., 2002. Zonal Load Estimation Studies in Radial Power Distribution Networks. *IEEE Int. Symp. on Circuits and Systems*, **5**:697-700. [doi:10.1109/ISCAS.2002.1010799]
- Wang, H.B., Schulz, N.N., 2004. A revised branch current-based distribution system state estimation algorithm and meter placement impact. *IEEE Trans. on Power Syst.*, **19**(1):207-213. [doi:10.1109/TPWRS.2003.821426]